

# Coalescing hardcore-boson condensate states with nonzero momentum

© C. H. Zhang and © Z. Song\*

School of Physics, Nankai University, Tianjin 300071, China

\* [songtc@nankai.edu.cn](mailto:songtc@nankai.edu.cn)

## Abstract

Exceptional points (EPs), as an exclusive feature of a non-Hermitian system, support coalescing states to be alternative stable state beyond the ground state. In this work, we explore the influence of non-Hermitian impurities on the dynamic formation of condensate states in one-, two-, and three-dimensional extended Bose-Hubbard systems with strong on-site interaction. Based on the solution for the hardcore limit, we show exactly that condensate modes with off-diagonal long-range order (ODLRO) can exist when certain system parameters satisfy specific matching conditions. Under open boundary conditions, the condensate states become coalescing states when the non-Hermitian  $\mathcal{PT}$ -symmetric boundary gives rise to the EPs. The fundamental mechanism behind this phenomenon is uncovered through analyzing the scattering dynamics of many-particle wavepackets at the non-Hermitian boundaries. The EP dynamics facilitate the dynamic generation of condensate states with non-zero momentum. To further substantiate the theoretical findings, numerical simulations are conducted. This study not only unveils the potential condensation of interacting bosons but also offers an approach for the engineering of condensate states.



Copyright C. H. Zhang and Z. Song.

This work is licensed under the Creative Commons

[Attribution 4.0 International License](https://creativecommons.org/licenses/by/4.0/).

Published by the SciPost Foundation.

Received 2024-07-03

Accepted 2024-12-10

Published 2025-01-31

doi:[10.21468/SciPostPhysCore.8.1.013](https://doi.org/10.21468/SciPostPhysCore.8.1.013)



Check for updates

## Contents

<b>1</b>	<b>Introduction</b>	<b>2</b>
<b>2</b>	<b>Model and condensate states</b>	<b>3</b>
<b>3</b>	<b>Coalescing condensate states</b>	<b>5</b>
<b>4</b>	<b>Resonant scattering of non-Hermitian impurity</b>	<b>6</b>
<b>5</b>	<b>Dynamic generation of condensate states</b>	<b>9</b>
<b>6</b>	<b>Summary</b>	<b>11</b>
<b>A</b>	<b>Condensate eigenstates with ODLRO</b>	<b>12</b>
<b>B</b>	<b>Coalescing condensate states</b>	<b>13</b>
	<b>References</b>	<b>14</b>

# 1 Introduction

Recent developments in cold atom experiments provide a versatile platform for realizing various phases of interacting and non-interacting bosonic systems [1–4]. Available experimental setups nowadays allow for the control of both geometry and interactions, so as to investigate the real-time evolution of quantum many-body systems directly with engineered model Hamiltonians [1, 5, 6]. It thus boosts the theoretical predictions of exotic quantum phases in interacting systems, which then might be realized and tested in experiments. Exact solutions for quantum many-body systems are rare, but important for providing valuable insights for the characterization of new forms of quantum matter and dynamic behaviors.

Bose-Einstein condensation (BEC) is one of the most striking manifestations of the quantum nature of matter on the macroscopic scale [7]. It represents a formation of a collective quantum state of free bosons. Intuitively, on-site repulsive interactions should block the formation of BEC under the moderate particle density. A lot of effort has been devoted to investigate and understand the role of particle-particle interactions on the occurrence of BEC [8, 9].

On the other hand, recent years have seen a growing interest in non-Hermitian descriptions of condensed-matter systems [10–26]. It has been shown that the interplay between non-Hermiticity and interaction can give rise to exotic quantum many-body effect, ranging from non-Hermitian extensions of Kondo effect [15, 27], many-body localization [21], Fermi surface in coordinate space [28], to fermionic superfluidity [18, 29]. The cooperation between the non-Hermiticity and interaction may lead to rich quantum phases due to the peculiarity of non-Hermitian system.

Exceptional points (EPs), as an exclusive feature of a non-Hermitian system, are degeneracies of non-Hermitian operators [30–33]. The corresponding eigenstates coalesce into one state, resulting in the incompleteness of Hilbert space. The peculiar features around EP have sparked tremendous attention to the classical and quantum photonic systems [34–40]. Notably, a coalescing state has an exclusive feature. On the one hand, it is an eigenstate of the Hamiltonian, on the other hand, it has the advantage that it is also a target state for a long-time evolution of various initial states. In this sense, a coalescing state is an alternative stable state beyond the ground state. Given the above rapidly growing fields in experimental and theoretical perspectives, we are motivated to investigate the impact of non-Hermitian impurities on the dynamic formation of condensate states of interacting bosons.

In this paper, we study one-, two-, and three-dimensional extended Bose-Hubbard systems with strong on-site interaction. The exact solution for the hardcore limit shows that there exists condensate modes when the system parameters meet the matching conditions. It also allows us to calculate the correlation function for any size system, so as to prove that condensate states indeed possesses off-diagonal long-range order (ODLRO) [41]. We focus on the impact of non-Hermitian impurities on the dynamic formation of condensate states. For open boundary condition, the condensate states become coalescing states when the non-Hermitian  $\mathcal{PT}$ -symmetric boundary induces the EPs. The underlying mechanism is revealed by the reflectionless absorption of many-particle wavepacket with resonant momentum by the non-Hermitian boundary. In parallel, the EP dynamics allows the dynamic generation of condensate states with nonzero momentum. We perform numerical simulations for finite-size system to demonstrate and verify the theoretical results. The finding not only reveals the possible condensation of interaction bosons, but also provides a method for condensate state engineering in an alternative way. The implications of this work are significant for both theoretical and practical applications in the realm of quantum many-body systems and could pave the way for innovative strategies in quantum state manipulation and control.

This paper is organized as follows. In Sec. 2, we introduce the model Hamiltonian and its condensate eigenstate. In Sec. 3, we derive the exact condition for coalescing condensate

state. In Sec. 4, we perform the numerical simulations to demonstrate reflectionless scattering of many-particle Gaussian wavepacket at non-Hermitian boundary. In Sec. 5, we present the possibility of dynamically generating condensate state with an arbitrary initial state. Finally, we summarize our results in Sec. 6.

## 2 Model and condensate states

We start our study from a general form of the Hamiltonian on a three-dimensional lattice  $N_1 \times N_2 \times N_3$

$$H = \sum_{\alpha=1}^3 J_{\alpha} \sum_{\mathbf{r}} \frac{1}{2} \hat{a}_{\mathbf{r}}^{\dagger} \hat{a}_{\mathbf{r}+\mathbf{e}_{\alpha}} + \text{H.c.} + \sum_{\alpha=1}^3 V_{\alpha} \sum_{\mathbf{r}} \hat{n}_{\mathbf{r}} \hat{n}_{\mathbf{r}+\mathbf{e}_{\alpha}} + \sum_{\alpha=1}^3 \sum_{\mathbf{r}} (\mu_{\alpha} \hat{n}_{\mathbf{r}} \delta_{1,m_{\alpha}} + \mu_{\alpha}^* \hat{n}_{\mathbf{r}} \delta_{N_{\alpha},m_{\alpha}}), \quad (1)$$

where  $\hat{a}_{\mathbf{r}}^{\dagger}$  is the hardcore boson creation operator at the position  $\mathbf{r} = m_1 \mathbf{e}_1 + m_2 \mathbf{e}_2 + m_3 \mathbf{e}_3$  ( $m_{\alpha} = 1, 2, \dots, N_{\alpha}$ ,  $\alpha = 1, 2, 3$ ), satisfying

$$\{\hat{a}_l, \hat{a}_l^{\dagger}\} = 1, \quad \{\hat{a}_l, \hat{a}_l\} = 0, \quad (2)$$

and

$$[\hat{a}_j, \hat{a}_l^{\dagger}] = 0, \quad [\hat{a}_j, \hat{a}_l] = 0, \quad (3)$$

for  $j \neq l$ , and  $\hat{n}_{\mathbf{r}} = \hat{a}_{\mathbf{r}}^{\dagger} \hat{a}_{\mathbf{r}}$ ,  $\mathbf{e}_{\alpha}$  is the unit vector for  $N_{\alpha}$ . Under the open boundary condition, we define  $\hat{a}_{\mathbf{r}+N_{\alpha}\mathbf{e}_{\alpha}} = 0$ , while  $\hat{a}_{\mathbf{r}+N_{\alpha}\mathbf{e}_{\alpha}} = \hat{a}_{\mathbf{r}}$  for the periodic boundary condition ( $\alpha = 1, 2, 3$ ).

The parameters are taken as

$$\begin{cases} V_{\alpha} = J_{\alpha} \cos q_{\alpha}, \\ \mu_{\alpha} = J_{\alpha} \frac{e^{iq_{\alpha}}}{2}, \end{cases} \quad (4)$$

with arbitrary real number  $q_{\alpha}$  for the case with open boundary condition, but with  $\mathbf{q} = (q_1, q_2, q_3)$ ,  $q_{\alpha} = 2\pi m_{\alpha}/N_{\alpha}$  ( $m_{\alpha} = 1, 2, \dots, N_{\alpha}$ ,  $\alpha = 1, 2, 3$ ) and  $\mu_{\alpha} = 0$  with periodic boundary condition. When taking  $\{N_{\alpha}\} = (N_1, N_2, N_3) = (N_1, N_2, 1)$  or  $(N_1, 1, 1)$ , the system reduces to two- or one-dimensional systems.

In the following, we will show that state

$$|\psi_n\rangle = \frac{1}{\Omega_n} \left( \sum_{\mathbf{r}} \hat{a}_{\mathbf{r}}^{\dagger} e^{-i\mathbf{q}\cdot\mathbf{r}} \right)^n |0\rangle, \quad (5)$$

$$\Omega_n = \frac{1}{(n!) \sqrt{C_N^n}}, \quad (6)$$

is an eigenstate of the system, where the vacuum state  $|0\rangle = \prod_{\mathbf{r}} |0\rangle_{\mathbf{r}}$ , with  $\hat{a}_{\mathbf{r}} |0\rangle_{\mathbf{r}} = 0$ . In both two cases (also including mixed boundary conditions), the Hamiltonian can be written as the form

$$H = \sum_{\alpha=1}^3 \sum_{\mathbf{r}} h_{\mathbf{r}}^{\alpha} + \sum_{\alpha=1}^3 V_{\alpha} \hat{n}_{\mathbf{r}}, \quad (7)$$

where the dimer term is non-Hermitian, i.e.,

$$h_{\mathbf{r}}^{\alpha} = J_{\alpha} \left[ \frac{1}{2} \hat{a}_{\mathbf{r}}^{\dagger} \hat{a}_{\mathbf{r}+\mathbf{e}_{\alpha}} + \text{H.c.} + \cos(\mathbf{q} \cdot \mathbf{e}_{\alpha}) (\hat{n}_{\mathbf{r}} \hat{n}_{\mathbf{r}+\mathbf{e}_{\alpha}} - \hat{n}_{\mathbf{r}} - \hat{n}_{\mathbf{r}+\mathbf{e}_{\alpha}}) + \frac{1}{2} (e^{i\mathbf{q}\cdot\mathbf{e}_{\alpha}} \hat{n}_{\mathbf{r}} + e^{-i\mathbf{q}\cdot\mathbf{e}_{\alpha}} \hat{n}_{\mathbf{r}+\mathbf{e}_{\alpha}}) \right], \quad (8)$$

and  $\hat{n} = \sum_{\mathbf{r}} \hat{n}_{\mathbf{r}}$  is the total number operator. It is easy to check that

$$\begin{aligned} h_{\mathbf{r}}^{\alpha} [e^{-i\mathbf{q}\cdot\mathbf{r}} \hat{a}_{\mathbf{r}}^{\dagger} + e^{-i\mathbf{q}\cdot(\mathbf{r}+\mathbf{e}_{\alpha})} \hat{a}_{\mathbf{r}+\mathbf{e}_{\alpha}}^{\dagger}] |0\rangle_{\mathbf{r}} |0\rangle_{\mathbf{r}+\mathbf{e}_{\alpha}} &= 0, \\ h_{\mathbf{r}}^{\alpha} \hat{a}_{\mathbf{r}}^{\dagger} \hat{a}_{\mathbf{r}+\mathbf{e}_{\alpha}}^{\dagger} |0\rangle_{\mathbf{r}} |0\rangle_{\mathbf{r}+\mathbf{e}_{\alpha}} &= 0, \\ h_{\mathbf{r}}^{\alpha} |0\rangle_{\mathbf{r}} |0\rangle_{\mathbf{r}+\mathbf{e}_{\alpha}} &= 0, \end{aligned} \quad (9)$$

which ensures that

$$H |\psi_n\rangle = n \sum_{\alpha=1}^3 V_\alpha |\psi_n\rangle . \quad (10)$$

To understand the underlying mechanism for the existence of such eigenstates, we consider a free boson model on an  $N$ -site ring with the following Hamiltonian

$$H_{\text{FB}} = \sum_{j=1}^N (\hat{b}_j^\dagger \hat{b}_{j+1} + \text{H.c.}) , \quad (11)$$

where  $b_j^\dagger$  and  $b_j$  are creation and annihilation operators for a boson on site  $j$ , respectively. We consider a two-boson eigenstate given by

$$|2, q\rangle = \left( \sum_{j=1}^N e^{iqj} \hat{b}_j^\dagger \right)^2 |0\rangle , \quad (12)$$

which satisfies the Schrodinger equation

$$H_{\text{FB}} |2, q\rangle = 4 \cos q |2, q\rangle . \quad (13)$$

We note that the state  $|2, q\rangle$  and the hardcore boson state

$$|\psi_2\rangle = \left( \sum_{j=1}^N e^{iqj} \hat{a}_j^\dagger \right)^2 |0\rangle , \quad (14)$$

have the relation

$$|2, q\rangle = |\psi_2\rangle + \sum_{j=1}^N e^{i2qj} (\hat{b}_j^\dagger)^2 |0\rangle . \quad (15)$$

The Eq. (13) can be explicitly written as

$$\begin{aligned} H_{\text{FB}} |2, q\rangle &= H_{\text{FB}} |\psi_2\rangle + H_{\text{FB}} \sum_{j=1}^N e^{i2qj} (\hat{b}_j^\dagger)^2 |0\rangle \\ &= H_{\text{FB}} |\psi_2\rangle + 4 \cos q \sum_{j=1}^N e^{iqj} e^{iq(j+1)} \hat{b}_j^\dagger \hat{b}_{j+1}^\dagger |0\rangle . \end{aligned} \quad (16)$$

The identity

$$\hat{b}_j^\dagger \hat{b}_{j+1}^\dagger |0\rangle = (\hat{b}_l^\dagger \hat{b}_l \hat{b}_{l+1}^\dagger \hat{b}_{l+1}) \hat{b}_j^\dagger \hat{b}_{j+1}^\dagger |0\rangle , \quad (17)$$

ensures

$$H_{\text{FB}} |2, q\rangle = H_{\text{FB}} |\psi_2\rangle + 2 \cos q \left( \sum_l \hat{b}_l^\dagger \hat{b}_l \hat{b}_{l+1}^\dagger \hat{b}_{l+1} \right) |2, q\rangle . \quad (18)$$

Then we have

$$H_{\text{FB}} |\psi_2\rangle + 2 \cos q \left( \sum_l \hat{b}_l^\dagger \hat{b}_l \hat{b}_{l+1}^\dagger \hat{b}_{l+1} \right) |2, q\rangle = 4 \cos q |2, q\rangle , \quad (19)$$

and furthermore

$$\left[ H_{\text{FB}} + 2 \cos q \left( \sum_l \hat{b}_l^\dagger \hat{b}_l \hat{b}_{l+1}^\dagger \hat{b}_{l+1} \right) \right] |\psi_2\rangle = 4 \cos q |2, q\rangle . \quad (20)$$

Applying the projection operator  $P$ , given by

$$P(\hat{b}_j^\dagger)^2 |0\rangle = 0, \quad (21)$$

to the above equation, we obtain the corresponding Schrodinger equation for the state  $|\psi_2\rangle$ . This operator can be realized by adding infinite on-site interaction, which rules out the doublon state  $(\hat{b}_j^\dagger)^2 |0\rangle$ . It is clear that the hardcore constraint forbids transitions from the state  $(\hat{b}_j^\dagger)^2 |0\rangle$  to states  $\hat{b}_{j-1}^\dagger \hat{b}_j^\dagger |0\rangle$  and  $\hat{b}_j^\dagger \hat{b}_{j+1}^\dagger |0\rangle$ . To compensate for these states, the resonant NN interaction can be introduced. In this sense, the resonant NN interaction serves to cancel out the effects from hardcore scattering.

In addition, state  $|\psi_n\rangle$  possesses ODLRO due to the fact that the correlation function

$$\langle \psi_n | \hat{a}_\mathbf{r}^\dagger \hat{a}_{\mathbf{r}+\mathbf{R}} | \psi_n \rangle = e^{-iq \cdot \mathbf{R}} \frac{(N-n)n}{N(N-1)}, \quad (22)$$

does not decay as  $|\mathbf{R}|$  increases. The detail derivation is given in the Appendix A. In the dilute case where  $n \ll N$ , the on-site and NN interactions can be neglected. The system can be regarded as a free boson system, exhibiting a superfluid state. However, in the case where  $n \sim N$ , the on-site and NN interactions are not negligible. In the extreme case, we have

$$|\psi_N\rangle \propto \frac{1}{\Omega_n} \prod_{\mathbf{r}} \hat{a}_\mathbf{r}^\dagger |0\rangle, \quad (23)$$

which is obviously an insulating state. This can be seen from the fact that the corresponding correlation function  $\langle \psi_N | \hat{a}_\mathbf{r}^\dagger \hat{a}_{\mathbf{r}+\mathbf{R}} | \psi_N \rangle$  vanishes.

### 3 Coalescing condensate states

In this section, we turn to investigate the unique feature, the EP, in the present non-Hermitian system described by Eq. (1). On the one hand, the strength of non-Hermitian impurities in the resonant Hamiltonian depends on the value of  $q$ . On the other hand, the discrete values of  $q$  can be adjusted by the size of the system. It is presumably the case that there exist some critical values of  $q$ , at which the Hamiltonian reaches the EP.

In parallel, without loss of generality, we have

$$|\varphi_n\rangle = \frac{1}{\Omega_n} \left( \sum_{\mathbf{r}} \hat{a}_\mathbf{r}^\dagger e^{iq \cdot \mathbf{r}} \right)^n |0\rangle, \quad (24)$$

for the equation

$$H^\dagger |\varphi_n\rangle = n \sum_{\alpha=1}^3 V_\alpha |\varphi_m\rangle, \quad (25)$$

which establishes the biorthonormal set  $\{|\varphi_m\rangle, |\psi_n\rangle\}$ , satisfying

$$\langle \varphi_m | \psi_n \rangle = \delta_{mn}, \quad (26)$$

except for some special cases. We start the demonstrations from the simplest case with  $n = 1$ . Straightforward derivation shows that

$$\langle \varphi_1 | \psi_1 \rangle = 0, \quad (27)$$

if  $q_\alpha = q_\alpha^c = \pi m_\alpha / N_\alpha$  ( $m_\alpha \in [1, 2N_\alpha - 1]$ ,  $m_\alpha \neq N_\alpha$ ) for any one of  $\alpha$ , which indicates that the complete set of eigenstates is spoiled. According to non-Hermitian quantum mechanics, the Hamiltonian with parameter  $q_\alpha^c$  has an EP and  $|\psi_1\rangle$  is referred to as a coalescing state. We note that an EP can be induced by the parameter along a single direction (any one of  $\alpha = 1, 2$ , and  $3$ ). In this sense, the conditions for occurrence of EP are independent of three directions. Then one can investigate the EP problem from a 1D system, which makes things easily accessible. However, it is not a straightforward conclusion that  $|\psi_n\rangle$  is a coalescing state simultaneously, since operator  $\hat{a}_\dagger$  obeys an unusual commutation relations in Eq. (4).

Considering a 1D system with a set of Hamiltonians in Eq. (1) with open boundary condition, i.e.,  $N_1 = N$ ,  $N_2 = N_3 = 1$ , and  $q_1^c = \pi m_1 / N = 2\pi m_1 / (2N)$  ( $m_1 \in [1, 2N - 1]$ ,  $m_1 \neq N$ ), each Hamiltonian  $H(q_1^c)$  is tuned at EP. The matrix representation of  $H(q_1^c)$  in the single-particle invariant subspace should have an EP [42, 43] due to the existence of  $2 \times 2$  Jordan block. A natural question is what happens in the  $n$ -particle invariant subspace and whether  $|\psi_n\rangle$  is also a coalescing state. To answer this question, we consider another set of Hamiltonians in Eq. (1) with periodic boundary condition, i.e.,  $N_1 = 2N$ ,  $N_2 = N_3 = 1$ , and  $q_1 = 2\pi m_1 / (2N)$  ( $m_1 \in [1, 2N]$ ). Each Hamiltonian  $H(q_1)$  is Hermitian and supports the Schrodinger equation

$$H(q_1)|\Psi_n\rangle = nV_1|\Psi_n\rangle, \quad (28)$$

with eigenstates

$$|\Psi_n\rangle = \frac{1}{\Omega_n} \left( \sum_{m=1}^{2N} \hat{a}_{me_1}^\dagger e^{-imq_1} \right)^n |0\rangle. \quad (29)$$

Notably, we find that the coalescing state  $|\psi_1\rangle$  of  $H(q_1^c)$  is exactly the half part of the eigenstate  $|\Psi_1\rangle$ . It is a starting point, based on which we can show that

$$\langle \varphi_n | \psi_n \rangle = 0, \quad (30)$$

i.e., state  $|\psi_n\rangle$  is also a coalescing state of the Hamiltonian  $H(q_1^c)$ . The detail derivation is given in the Appendix B. It has been shown that non-Hermitian impurities have an intimate relationship with the scattering solutions of Hermitian systems [44–46]. In comparison with previous studies, the coalescing states obtained in this work not only provide an exact example but also extend the investigation to many-body systems.

## 4 Resonant scattering of non-Hermitian impurity

In this section, we focus on our study on 1D system for simplicity. The obtained result can be extended to 2D and 3D systems. We start with our investigation on the Hamiltonian in a single-particle invariant subspace, in which the single-particle dynamics obeys a free boson model with the  $\mathcal{PT}$  symmetric non-Hermitian Hamiltonian

$$H_{\text{FB}} = \sum_{j=1}^{N-1} \left( \hat{b}_j^\dagger \hat{b}_{j+1} + \text{H.c.} \right) + e^{-iq} \hat{b}_1^\dagger \hat{b}_1 + e^{iq} \hat{b}_N^\dagger \hat{b}_N, \quad (31)$$

on an  $N$ -site chain with complex on-site potential at two ends. We take a dimensionless constant for the sake of simplicity. According to the analysis in last two sections, states

$$\left( \sum_{j=1}^N e^{iqj} \hat{b}_j^\dagger \right)^n |0\rangle, \quad (32)$$

are  $n$ -boson eigenstates of  $H_{\text{FB}}$ . In addition, these states with different  $n$  are coalescing states under the condition  $q = q_c = \pi m / N$  ( $m \in [1, 2N - 1]$ ,  $m \neq N$ ). Furthermore, this constraint

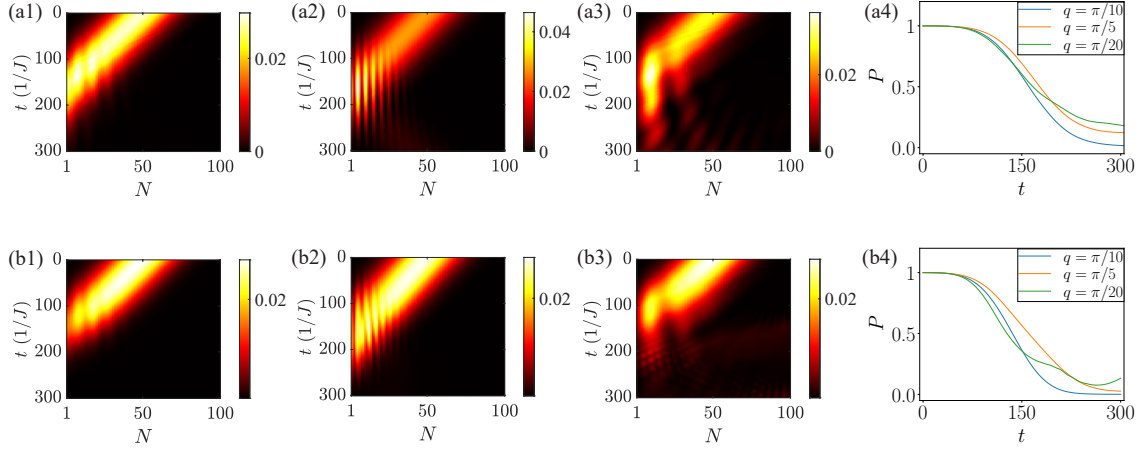


Figure 1: Plots of  $p_j(t)$  and  $P(t)$  defined in Eqs. (40) and (41) for the initial states defined in Eq. (39) with  $n = 1$  in (a1)-(a4) and  $n = 2$  in (b1)-(b4), respectively. The parameters of the Gaussian wavepacket are  $\alpha = 0.05$ ,  $N_0 = 50$  and  $q = \pi/10$  in (a1, b1),  $\pi/5$  in (a2, b2),  $\pi/20$  in (a3, b3). The system parameter is  $q_c = \pi/10$ . The profiles of  $p_j(t)$  in (a2, b2, a3, b3) exhibit evident interference fringes indicating reflections from the end of the chain. The plots of  $P(t)$  indicate the perfect probability absorption for the resonant incident wavepackets.

for  $q_c$  is satisfied automatically in large  $N$  limit. It has been shown that this fact has intimate connection to the reflectionless scattering problem [43] for the semi-infinite system

$$H_{\text{FB}}^{\infty} = \sum_{j=1}^{\infty} (\hat{b}_j^{\dagger} \hat{b}_{j+1} + \text{H.c.}) + e^{-iq_c} \hat{b}_1^{\dagger} \hat{b}_1, \quad (33)$$

with a complex impurity at the end. The dynamic demonstration of this exact result is the near-perfect reflectionless of a Gaussian wavepacket with resonant momentum  $q = q_c$ . Specifically, we consider an initial  $n$ -boson state in the form

$$|\phi(0)\rangle = \left( \sum_j g_j \hat{b}_j^{\dagger} \right)^n |0\rangle, \quad (34)$$

where the single-boson wave function has the form

$$g_j = e^{-\frac{\alpha^2}{2}(j-N_0)^2} e^{iqj}. \quad (35)$$

The shape and center of the wavepacket are determined by parameters  $\alpha$  and  $N_0$ . The near-perfect reflectionless indicates the time evolution of  $|\phi(0)\rangle$  obeys

$$\lim_{t \rightarrow \infty} e^{-iH_{\text{FB}}^{\infty} t} |\phi(0)\rangle \approx 0. \quad (36)$$

It holds true for any  $n$  with small  $\alpha$ , due to the following facts. (i) A wider single-boson wavepacket with  $q = q_c$  can reflect the exact result for plane wave scattering from the end [43]. (ii) Multi-boson wavepacket shares the same dynamic behavior of a single-boson, since there is no interaction between bosons.

Now we turn to the hardcore boson Hubbard model, by ruling out the double occupation and adding the resonant NN interaction with the Hamiltonian

$$H_{\text{HB}}^{\infty} = \sum_{j=1}^{\infty} (\hat{a}_j^{\dagger} \hat{a}_{j+1} + \text{H.c.} + 2 \cos q_c \hat{n}_j \hat{n}_{j+1}) + e^{-iq_c} \hat{a}_1^{\dagger} \hat{a}_1. \quad (37)$$

The question is whether we still have the result

$$\lim_{t \rightarrow \infty} e^{-iH_{\text{HB}}^{\infty} t} \left( \sum_j g_j \hat{a}_j^{\dagger} \right)^n |0\rangle \approx 0, \quad (38)$$

for the initial state

$$|\phi(0)\rangle = \left( \sum_j g_j \hat{a}_j^{\dagger} \right)^n |0\rangle. \quad (39)$$

To answer this question, numerical simulations are performed for the  $n$ -hardcore-boson initial wavepackets  $|\phi(0)\rangle$  with  $q$  around  $q_c$ . The evolved states  $|\phi(t)\rangle = e^{-iH_{\text{HB}} t} |\phi(0)\rangle$  are computed by exact diagonalization for finite systems with several typical set of parameters.

The profiles of the evolved states and the total probabilities are measured by

$$p_j(t) = \left| \frac{\hat{a}_j |\phi(t)\rangle}{|\phi(0)\rangle} \right|^2 = \left| \frac{\hat{a}_j e^{-iH_{\text{HB}}^{\infty} t} |\phi(0)\rangle}{|\phi(0)\rangle} \right|^2, \quad (40)$$

and

$$P(t) = \frac{1}{n} \sum_j p_j(t) = \left| \frac{e^{-iH_{\text{HB}}^{\infty} t} |\phi(0)\rangle}{|\phi(0)\rangle} \right|^2, \quad (41)$$

respectively.

We plot the two quantities  $p_j(t)$  and  $P(t)$  in Fig. 1(a) and (b) for selected systems with two types of initial states. The parameters of the initial wavepackets and the driven systems are given in the captions of the figure. We consider the driven Hamiltonians on a finite site chain with the parameter  $q_c = \pi/10$ . The initial states are taken as: (a) a single-boson wavepacket and (b) a two-boson wavepacket, respectively. The center momenta of the wavepackets are taken as  $q = q_c, q_c/2$ , and  $2q_c$ , respectively. According to the analysis above, both the single- and two-boson incident wavepackets with the resonant momentum  $q_c$  should be approximately absorbed by the ending non-Hermitian impurity. From Fig. 1(a1)-(a3), one can observe that there is no reflection pattern in (a1) for the resonant wavepacket. In contrast, evident interference fringes are observed near the end of the chain in cases (a2) and (a3), where the incident wavepackets are off-resonant. Such patterns result from the interference between incident and reflected wavepackets. From Fig. 1(a4), one can see that the probabilities for each case reduce significantly when the wavepackets reach the impurity, exhibiting absorption behavior. Notably, the absorption is minimal when the initial wavepacket carries the resonant momentum  $q_c$ . This result is consistent with the patterns observed in Fig. 1(a1)-(a3). Actually, the plots in Fig. 1(a1)-(a4) are provided to compare the results with those for two-boson incident wavepackets, which are shown in Fig. 1(b1)-(b4). We observe that the two sets of patterns have the similar profiles. The results indicate perfect absorption for resonant incident wavepackets with  $q = q_c$  in both the one- and two-boson cases, which is in accordance with the previous theoretical analysis. Then, on the one hand, the results indicate that the underlying mechanism for the coalescing condensate states in an open chain is the reflectionless absorption of many-particle wavepackets with resonant momentum by the non-Hermitian boundary. These resonant absorptions demonstrate the dynamic signature of the EP. On the other hand, it reveals an interesting dynamic behavior of a many-particle wavepacket: it behaves as a single-particle wavepacket. The NN resonant interaction indeed plays a role in canceling out the scattering effect arising from the hardcore interaction.

Table 1: The structures of energy levels for 10-site open chain with different  $q$  and filling particle number  $n$ . We list the numbers of coalescing states  $n_{CS}$ , of order  $n_{OR}$ , and the numbers of complex levels  $n_{CM}$  in the form  $(n_{CM}, n_{OR} \times n_{CS})$ . It indicates that all the energy levels are real and all the systems contain 2-order coalescing states.

$q$	$n=2$	3	4	5
$\pi/10$	$0, 2 \times 1$	$0, 2 \times 1$	$0, 2 \times 1$	$0, 2 \times 1$
$2\pi/10$	$0, 2 \times 1$	$0, 2 \times 1$	$0, 2 \times 36$	$0, 2 \times 43$
$3\pi/10$	$0, 2 \times 1$	$0, 2 \times 1$	$0, 2 \times 1$	$0, 2 \times 1$
$4\pi/10$	$0, 2 \times 1$	$0, 2 \times 1$	$0, 2 \times 36$	$0, 2 \times 43$

Table 2: The same as Table 1 but for  $N_1 \times N_2 = 5 \times 3$  lattice with different  $(q_1, q_2)$ . We take open boundary condition in  $q_1$ -direction and periodic boundary condition in  $q_2$ -direction. It indicates that all the systems contain complex levels and multiple 2-order coalescing states.

$(q_1, q_2)$	$n=2$	3	4
$(\pi/5, 2\pi/3)$	$7, 2 \times 11$	$135, 2 \times 5$	$525, 2 \times 2$
$(2\pi/5, 2\pi/3)$	$16, 2 \times 11$	$173, 2 \times 5$	$586, 2 \times 2$
$(3\pi/5, 2\pi/3)$	$16, 2 \times 11$	$171, 2 \times 5$	$586, 2 \times 2$
$(4\pi/5, 2\pi/3)$	$13, 2 \times 11$	$159, 2 \times 5$	$570, 2 \times 2$

## 5 Dynamic generation of condensate states

Condensate state as macroscopic quantum state has significance both in theoretical and experimental physics. The stability of such states is crucial in practice. In general, it can be prepared as ground state by decreasing the temperature. Dynamical generation of nonequilibrium steady condensate states is another way, which has been received much attention recently. The advantage of an EP system is that a coalescing state is also a target state for a long-time evolution of various initial states. In the above, we have shown that the state  $|\psi_n\rangle$  is also a coalescing state of the Hamiltonian  $H(q_1^c)$ . However, the order of EP is unknown, maybe depends on the particle numbers  $n$ , and the numbers of dimensions  $n_d$  at which the resonant boundary is taken.

In contrast, the order of EP for free boson model can be exactly obtained. In a single-boson invariant subspace, the maximal order of EP is  $n_d$ , and then is  $m$  for  $n$ -boson system, where

$$m = \frac{(n_d + n - 1)!}{n!(n_d - 1)!}. \quad (42)$$

According to the non-Hermitian quantum theory, there is a  $m$ -D Jordan block  $M$  in the matrix representation of the Hamiltonian, which ensures that

$$M^m = 0. \quad (43)$$

The dynamics for any state in this subspace of Jordan block, referred to as auxiliary states, is governed by the time evolution operator

$$U(t) = e^{-iEt} e^{-iMt} = e^{-iEt} \sum_{l=0}^{m-1} \frac{1}{l!} (-iMt)^l, \quad (44)$$

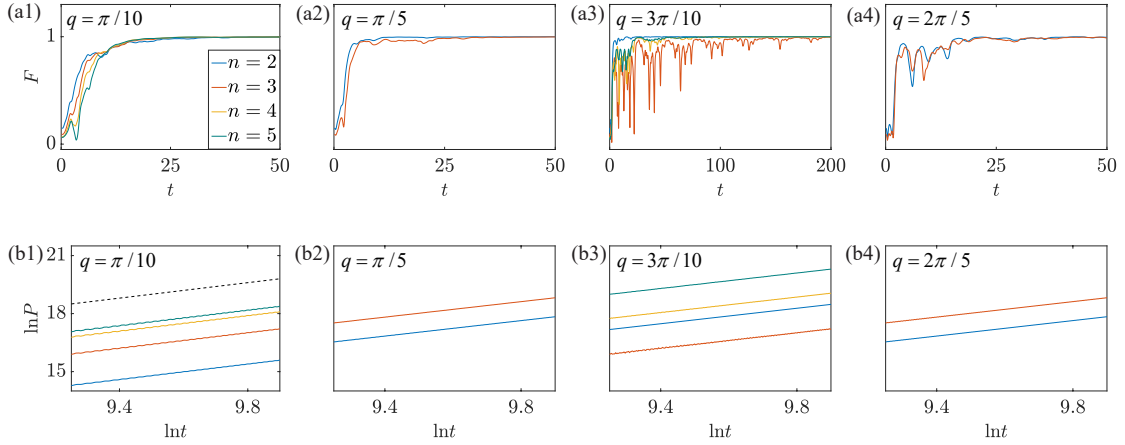


Figure 2: (a1)-(a4) present the time evolution of fidelity of  $n$ -particle one-dimensional system with  $q = m\pi/N$  where  $m$  ranges from 1 to 4. (b1)-(b4) present the time evolution of probability of the same system. The slope of dashed line as reference is 2 and it is nearly parallel to other colored lines. Here we only plot the results with a single 2-order coalescing state. The initial state is  $\prod_{j=1}^n \hat{a}_j^\dagger |0\rangle$  and the size of system  $N = 10$ , where the number  $n$  is indicated in the panel. The results show that the unentangled initial states can indeed evolve to the corresponding target with high fidelity.

where  $E$  is a constant without any effect on the evolved state. It indicates that for an initial state  $|\phi(0)\rangle$  involving the auxiliary states we have  $|\phi(t)\rangle = U(t)|\phi(0)\rangle$

$$\lim_{t \rightarrow \infty} |\phi(t)\rangle \propto \left( \sum_{\mathbf{r}} e^{-i\mathbf{q}\cdot\mathbf{r}} \hat{b}_{\mathbf{r}}^\dagger \right)^n |0\rangle, \quad (45)$$

within large  $t$  region and

$$\| |\phi(t)\rangle \|^2 \propto t^{2(m-1)}, \quad (46)$$

which is also a dynamic demonstration for the order of the Jordan block.

However, such an analysis may be invalid due to the particle-particle interactions, i.e., replacing  $\hat{b}_{\mathbf{r}}^\dagger$  by  $\hat{a}_{\mathbf{r}}^\dagger$ . In this situation, numerical simulations for finite size systems can shed some light on the dynamic generation of the condensate states of hardcore bosons.

We perform numerical simulations on finite systems with the following considerations. (i) The analysis above only predicts the results within large time domain. The efficiency of the scheme should be estimated from numerical simulations. (ii) The final state seems to be independent of the initial states, which can be simply unentangled  $n$ -boson initial states in the form  $|\phi(0)\rangle = \prod_{\{l_1, l_2, \dots, l_j, \dots, l_n\}} \hat{a}_{l_j}^\dagger |0\rangle$ . (iii) The order of EP can be observed by the dynamic process. The energy levels of many-particle non-Hermitian system are complicated, containing complex energy levels and multiple coalescing states, which may pose an obstacle in the calculation of time evolution. Our strategy has two steps. First, we find out the structure of energy level for sample systems. Second, select several coalescing states as target states. In Tables 1 and 2, the numbers of complex energy and coalescing levels are listed. In general, the structure of energy levels is characterized by three integers, the number of coalescing states  $n_{CS}$ , the order  $n_{OR}$ , and the number of complex levels  $n_{CM}$ . These results guide numerical simulations. To demonstrate this scheme, the system should contain only real levels and a coalescing state. We select several cases that satisfy the condition to perform the computations.

The evolved states  $|\phi(t)\rangle$  are also computed by exact diagonalization for finite systems with several typical set of parameters. We focus on the Dirac probability  $P(t)$  defined in Eq. (41) and the fidelity

$$F(t) = \frac{|\langle\psi_n|\phi(t)\rangle|^2}{\|\phi(t)\|^2}, \quad (47)$$

which is the measure of the distance between the final state and the condensate states  $|\psi_n(q)\rangle$ .

We plot the fidelity  $F(t)$  in Fig. 2 as a function of  $t$  for selected systems and many-particle initial states. We consider the driven Hamiltonians on 10-site chains with the system parameters  $q = m\pi/10$ , where  $m$  ranges from 1 to 4. For  $m = 1$  and 3, we consider the sectors with  $n = 2, 3, 4$ , and 5. For  $m = 2$  and 4, we only consider the sectors with  $n = 2$  and 3. According to the results listed in Tables 1, the corresponding energy levels are all real and the systems contain only one 2-order EP, with the coalescing condensate states in the form

$$|\psi_n\rangle = \frac{1}{\Omega_n} \left( \sum_{j=1}^{10} \hat{a}_j^\dagger e^{-im\pi j/10} \right)^n |0\rangle. \quad (48)$$

The  $n$ -boson initial states are taken in the explicit form

$$|\phi(0)\rangle = \hat{a}_1^\dagger |0\rangle, \quad \hat{a}_1^\dagger \hat{a}_2^\dagger |0\rangle, \quad \hat{a}_1^\dagger \hat{a}_2^\dagger \hat{a}_3^\dagger |0\rangle, \quad \hat{a}_1^\dagger \hat{a}_2^\dagger \hat{a}_3^\dagger \hat{a}_4^\dagger |0\rangle, \quad \hat{a}_1^\dagger \hat{a}_2^\dagger \hat{a}_3^\dagger \hat{a}_4^\dagger \hat{a}_5^\dagger |0\rangle, \quad (49)$$

which is a trivial unentangled state and can be easily prepared in the experiment. From Fig. 2(a1)-(a4), one can see that the fidelities  $F(t)$  obtained by numerical simulations for these selected cases approach 1 as time increases. The fact that  $F(t) = 1$  indicates that the evolved state is identical to the target state. In addition, we also plot the probability  $P(t)$  as a function of time  $t$  to demonstrate the EP dynamic behavior. According to the analysis above, the probability should obey the relation  $P(t) \sim t^2$ . From Fig. 2 (b1)-(b4), one can see that the plots are close to the lines in the  $\ln P(t)$ - $\ln t$  plane, and the slopes are all approximately equal to 2. On the one hand, the results indicate that the target states given in Eq. (48) can be obtained through the time evolution of the given initial state  $|\phi(0)\rangle$ . On the other hand, the underlying mechanism of such dynamic preparation of a coalescing condensate state is the 2-order EP dynamics, which exhibit parabolas in the probability growth.

## 6 Summary

In summary, we have studied the Hermitian and non-Hermitian extended hardcore Bose-Hubbard model on one-, two-, and three-dimensional lattices. A set of exact eigenstates are constructed and have the following implications: (i) The strong on-site repulsion and nearest neighboring interaction cannot block the formation of BEC under the moderate particle density, when two interacting strengths are matched with each other. (ii) The solutions for Hermitian systems with periodic boundary condition are available for any given size, in which the momentum of the condensate is nothing but the reciprocal vector. Then the resonant non-Hermitian impurities can result in coalescing hardcore-boson condensate states. As an alternative stable state beyond the ground state, a coalescing state may be obtained via natural time evolution, although it is also the excited eigenstate of the system. In this sense, our finding not only reveals the possible condensation of interaction bosons, but also provides a method for condensate state engineering in an alternative way.

## Acknowledgments

**Funding information** This work was supported by the National Natural Science Foundation of China (under Grant No. 12374461).

## A Condensate eigenstates with ODLRO

In this appendix, we present the derivations on the eigenstates of the Hamiltonian in Eq. (1) and resonant conditions for many-body coalescing states. Consider the state

$$|\psi_n\rangle = \frac{1}{\Omega_n} \left( [e^{-i\mathbf{q}\cdot\mathbf{r}}\hat{a}_{\mathbf{r}}^\dagger + e^{-i\mathbf{q}\cdot(\mathbf{r}+\mathbf{R})}\hat{a}_{\mathbf{r}+\mathbf{R}}^\dagger] + A \right)^n |0\rangle, \quad (\text{A.1})$$

where  $A$  is an operator which does not contain  $\hat{a}_{\mathbf{r}}^\dagger$  and  $\hat{a}_{\mathbf{r}+\mathbf{R}}^\dagger$ . We have

$$|\psi_n\rangle = \frac{1}{\Omega_n} \sum_{k=1}^n C_n^k A^{n-k} [e^{-i\mathbf{q}\cdot\mathbf{r}}\hat{a}_{\mathbf{r}}^\dagger + e^{-i\mathbf{q}\cdot(\mathbf{r}+\mathbf{R})}\hat{a}_{\mathbf{r}+\mathbf{R}}^\dagger]^n |0\rangle. \quad (\text{A.2})$$

In fact, we note that

$$[e^{-i\mathbf{q}\cdot\mathbf{r}}\hat{a}_{\mathbf{r}}^\dagger + e^{-i\mathbf{q}\cdot(\mathbf{r}+\mathbf{R})}\hat{a}_{\mathbf{r}+\mathbf{R}}^\dagger]^2 |0\rangle = 2e^{-i\mathbf{q}\cdot(2\mathbf{r}+\mathbf{R})}\hat{a}_{\mathbf{r}}^\dagger\hat{a}_{\mathbf{r}+\mathbf{R}}^\dagger |0\rangle,$$

but

$$[e^{-i\mathbf{q}\cdot\mathbf{r}}\hat{a}_{\mathbf{r}}^\dagger + e^{-i\mathbf{q}\cdot(\mathbf{r}+\mathbf{R})}\hat{a}_{\mathbf{r}+\mathbf{R}}^\dagger]^k |0\rangle = 0 \quad (k > 2). \quad (\text{A.3})$$

Then

$$|\psi_n\rangle = \frac{1}{\Omega_n} \{A^n + nA^{n-1} [e^{-i\mathbf{q}\cdot\mathbf{r}}\hat{a}_{\mathbf{r}}^\dagger + e^{-i\mathbf{q}\cdot(\mathbf{r}+\mathbf{R})}\hat{a}_{\mathbf{r}+\mathbf{R}}^\dagger] + e^{-i\mathbf{q}\cdot(2\mathbf{r}+\mathbf{R})}n(n-1)A^{n-2}\hat{a}_{\mathbf{r}}^\dagger\hat{a}_{\mathbf{r}+\mathbf{R}}^\dagger\} |0\rangle. \quad (\text{A.4})$$

One can take  $\mathbf{R} = \mathbf{e}_\alpha$ , and then we have

$$h_{\mathbf{r}}^\alpha |\psi_n\rangle = 0, \quad (\text{A.5})$$

which ensures that

$$H |\psi_n\rangle = n \sum_{\alpha=1}^3 V_\alpha |\psi_n\rangle. \quad (\text{A.6})$$

Furthermore, we have

$$\begin{aligned} \hat{a}_{\mathbf{r}}^\dagger\hat{a}_{\mathbf{r}+\mathbf{R}} |\psi_n\rangle &= \frac{1}{\Omega_n} \{nA^{n-1} [e^{-i\mathbf{q}\cdot\mathbf{r}}\hat{a}_{\mathbf{r}}^\dagger\hat{a}_{\mathbf{r}+\mathbf{R}}\hat{a}_{\mathbf{r}}^\dagger + e^{-i\mathbf{q}\cdot(\mathbf{r}+\mathbf{R})}\hat{a}_{\mathbf{r}}^\dagger\hat{a}_{\mathbf{r}+\mathbf{R}}\hat{a}_{\mathbf{r}+\mathbf{R}}^\dagger]\} |0\rangle \\ &= \frac{1}{\Omega_n} nA^{n-1} e^{-i\mathbf{q}\cdot(\mathbf{r}+\mathbf{R})}\hat{a}_{\mathbf{r}}^\dagger |0\rangle, \end{aligned} \quad (\text{A.7})$$

which results in the correlation function

$$\begin{aligned} \langle \psi_n | \hat{a}_{\mathbf{r}}^\dagger\hat{a}_{\mathbf{r}+\mathbf{R}} | \psi_n \rangle &= \left( \frac{n}{\Omega_n} \right)^2 e^{-i\mathbf{q}\cdot\mathbf{R}} |A^{n-1} |0\rangle|^2 \\ &= e^{-i\mathbf{q}\cdot\mathbf{R}} \frac{(N-n)n}{N(N-1)}. \end{aligned} \quad (\text{A.8})$$

We find that

$$\lim_{|\mathbf{R}| \rightarrow \infty} |\langle \psi_n | \hat{a}_{\mathbf{r}}^\dagger\hat{a}_{\mathbf{r}+\mathbf{R}} | \psi_n \rangle| = \frac{n(N_1N_2N_3 - n)}{N_1N_2N_3(N_1N_2N_3 - 1)}, \quad (\text{A.9})$$

which is finite number, indicating off-diagonal long-range order (ODLRO) according to [41].

## B Coalescing condensate states

We start with the case with  $n = 1$ . The biorthogonal norm for state  $|\psi_1\rangle$  is

$$\begin{aligned} \langle \varphi_1 | \psi_1 \rangle &= \frac{1}{\Omega_n^2} \sum_{\mathbf{r}} e^{-i2\mathbf{q}\cdot\mathbf{r}} \\ &= \frac{1}{\Omega_n^2} \prod_{\alpha=1,2,3} \sum_{m_\alpha} e^{-i2q_\alpha m_\alpha}. \end{aligned} \quad (\text{B.1})$$

We note that if

$$\sum_{m_\alpha} e^{-i2q_\alpha m_\alpha} = 0, \quad (\text{B.2})$$

for one of  $\alpha$ , we have

$$\langle \varphi_1 | \psi_1 \rangle = 0, \quad (\text{B.3})$$

i.e., an EP can be induced by the parameter along a single direction.

In the following, we will show that it is also true for the case with  $n > 1$ . We only consider 1D systems for the sake of simplicity. We focus on two Hamiltonians. The first one is

$$H_{\text{HB}}^1 = \sum_{j=1}^{N-1} \left( \hat{a}_j^\dagger \hat{a}_{j+1} + \text{H.c.} + \cos q \hat{n}_j \hat{n}_{j+1} \right) + e^{-iq} \hat{a}_1^\dagger \hat{a}_1 + e^{iq} \hat{a}_N^\dagger \hat{a}_N, \quad (\text{B.4})$$

which is non-Hermitian and reduced from Eq. (1) for an  $N$ -site chain. The second one is

$$H_{\text{HB}}^2 = \sum_{j=1}^{2N} \left( \hat{a}_j^\dagger \hat{a}_{j+1} + \text{H.c.} + \cos q \hat{n}_j \hat{n}_{j+1} \right), \quad (\text{B.5})$$

which is Hermitian and reduced from Eq. (1) for a  $2N$ -site ring. Defining a set of collective operators

$$A^+ = \frac{1}{\sqrt{N}} \sum_{j=1}^N \hat{a}_j^\dagger e^{-iqj}, \quad B^+ = \frac{1}{\sqrt{N}} \sum_{j=N+1}^{2N} \hat{a}_j^\dagger e^{-iqj}, \quad (\text{B.6})$$

and

$$A^- = \frac{1}{\sqrt{N}} \sum_{j=1}^N \hat{a}_j e^{-iqj}, \quad B^- = \frac{1}{\sqrt{N}} \sum_{j=N+1}^{2N} \hat{a}_j e^{-iqj}, \quad (\text{B.7})$$

with  $q = 2\pi m / (2N)$  ( $m \in [1, 2N - 1]$ ,  $m \neq N$ ), a subset of the eigenstates of  $H_{\text{HB}}^1$  can be expressed as

$$|\psi_n\rangle = \frac{1}{\Lambda_n} (A^+)^n |0\rangle, \quad (\text{B.8})$$

while states

$$|\Psi_n\rangle = \frac{1}{\Lambda'_n} (A^+ + B^+)^n |0\rangle, \quad (\text{B.9})$$

and

$$|\Psi_n^*\rangle = \frac{1}{\Omega'_n} [(A^+ + B^+)^*]^n |0\rangle, \quad (\text{B.10})$$

are a subset of the eigenstates of  $H_{\text{HB}}^2$ , here

$$\Lambda_n = \frac{N^{n/2}}{(n!) \sqrt{C_N^n}}, \quad \Lambda'_n = \frac{N^{n/2}}{(n!) \sqrt{C_{2N}^n}}. \quad (\text{B.11})$$

We note that state  $|\psi_n\rangle$  is a part of state  $|\Psi_n\rangle$ , which is crucial for the following proof. The orthogonality of two states  $|\Psi_n\rangle$  and  $|\Psi_n^*\rangle$  leads to

$$\langle\Psi_n^*|\Psi_n\rangle = \sum_{m=0}^n p_m \langle 0|(A^-)^{n-m}(B^-)^m(A^+)^{n-m}(B^+)^m|0\rangle = 0. \quad (\text{B.12})$$

Taking  $n = 1$ , we have

$$\langle 0|(A^-A^+ + B^-B^+)|0\rangle = 0, \quad (\text{B.13})$$

which results in

$$\langle 0|A^-A^+|0\rangle = \langle 0|B^-B^+|0\rangle = 0, \quad (\text{B.14})$$

due to the translational symmetry of state  $|\Psi_n\rangle$ . Based on this conclusion, taking  $n = 2$ , we have  $\langle 0|(B^-B^+)^2|0\rangle = \langle 0|(A^-A^+)^2|0\rangle = 0$ . Furthermore, it turns out that

$$\langle 0|(A^-A^+)^m|0\rangle = 0, \quad (\text{B.15})$$

for  $m \in [0, n]$ , which results in

$$\langle\varphi_n|\psi_n\rangle = 0. \quad (\text{B.16})$$

## References

- [1] I. Bloch, J. Dalibard and S. Nascimbène, *Quantum simulations with ultracold quantum gases*, Nat. Phys. **8**, 267 (2012), doi:[10.1038/nphys2259](https://doi.org/10.1038/nphys2259).
- [2] M. Atala, M. Aidelsburger, M. Lohse, J. T. Barreiro, B. Paredes and I. Bloch, *Observation of chiral currents with ultracold atoms in bosonic ladders*, Nat. Phys. **10**, 588 (2014), doi:[10.1038/nphys2998](https://doi.org/10.1038/nphys2998).
- [3] M. Aidelsburger, M. Lohse, C. Schweizer, M. Atala, J. T. Barreiro, S. Nascimbène, N. R. Cooper, I. Bloch and N. Goldman, *Measuring the Chern number of Hofstadter bands with ultracold bosonic atoms*, Nat. Phys. **11**, 162 (2014), doi:[10.1038/nphys3171](https://doi.org/10.1038/nphys3171).
- [4] B. K. Stuhl, H.-I. Lu, L. M. Aycock, D. Genkina and I. B. Spielman, *Visualizing edge states with an atomic Bose gas in the quantum Hall regime*, Science **349**, 1514 (2015), doi:[10.1126/science.aaa8515](https://doi.org/10.1126/science.aaa8515).
- [5] E. Jané, G. Vidal, W. Dür, P. Zoller and J. I. Cirac, *Simulation of quantum dynamics with quantum optical systems*, Quantum Inf. Comput. **3**, 15 (2003), doi:[10.26421/QIC3.1-2](https://doi.org/10.26421/QIC3.1-2).
- [6] R. Blatt and C. F. Roos, *Quantum simulations with trapped ions*, Nat. Phys. **8**, 277 (2012), doi:[10.1038/nphys2252](https://doi.org/10.1038/nphys2252).
- [7] S. Bose, *Plancks Gesetz und Lichtquantenhypothese*, Z. Phys. **26**, 178 (1924), doi:[10.1007/BF01327326](https://doi.org/10.1007/BF01327326).
- [8] H. Shi, *Finite-temperature excitations in a dilute Bose-condensed gas*, Phys. Rep. **304**, 1 (1998), doi:[10.1016/S0370-1573\(98\)00015-5](https://doi.org/10.1016/S0370-1573(98)00015-5).
- [9] J. Andersen, *Theory of the weakly interacting Bose gas*, Rev. Mod. Phys. **76**, 599 (2004), doi:[10.1103/RevModPhys.76.599](https://doi.org/10.1103/RevModPhys.76.599).
- [10] T. E. Lee, *Anomalous edge state in a non-Hermitian lattice*, Phys. Rev. Lett. **116**, 133903 (2016), doi:[10.1103/PhysRevLett.116.133903](https://doi.org/10.1103/PhysRevLett.116.133903).

- [11] F. K. Kunst, E. Edvardsson, J. C. Budich and E. J. Bergholtz, *Biorthogonal bulk-boundary correspondence in non-Hermitian systems*, Phys. Rev. Lett. **121**, 026808 (2018), doi:[10.1103/PhysRevLett.121.026808](https://doi.org/10.1103/PhysRevLett.121.026808).
- [12] S. Yao, F. Song and Z. Wang, *Non-Hermitian Chern bands*, Phys. Rev. Lett. **121**, 136802 (2018), doi:[10.1103/PhysRevLett.121.136802](https://doi.org/10.1103/PhysRevLett.121.136802).
- [13] Z. Gong, Y. Ashida, K. Kawabata, K. Takasan, S. Higashikawa and M. Ueda, *Topological phases of non-Hermitian systems*, Phys. Rev. X **8**, 031079 (2018), doi:[10.1103/PhysRevX.8.031079](https://doi.org/10.1103/PhysRevX.8.031079).
- [14] R. El-Ganainy, K. G. Makris, M. Khajavikhan, Z. H. Musslimani, S. Rotter and D. N. Christodoulides, *Non-Hermitian physics and  $\mathcal{PT}$  symmetry*, Nat. Phys. **14**, 11 (2018), doi:[10.1038/nphys4323](https://doi.org/10.1038/nphys4323).
- [15] M. Nakagawa, N. Kawakami and M. Ueda, *Non-Hermitian Kondo effect in ultracold alkaline-earth atoms*, Phys. Rev. Lett. **121**, 203001 (2018), doi:[10.1103/PhysRevLett.121.203001](https://doi.org/10.1103/PhysRevLett.121.203001).
- [16] H. Shen and L. Fu, *Quantum oscillation from in-gap states and a non-Hermitian Landau level problem*, Phys. Rev. Lett. **121**, 026403 (2018), doi:[10.1103/PhysRevLett.121.026403](https://doi.org/10.1103/PhysRevLett.121.026403).
- [17] Y. Wu, W. Liu, J. Geng, X. Song, X. Ye, C.-K. Duan, X. Rong and J. Du, *Observation of parity-time symmetry breaking in a single-spin system*, Science **364**, 878 (2019), doi:[10.1126/science.aaw8205](https://doi.org/10.1126/science.aaw8205).
- [18] K. Yamamoto, M. Nakagawa, K. Adachi, K. Takasan, M. Ueda and N. Kawakami, *Theory of non-Hermitian fermionic superfluidity with a complex-valued interaction*, Phys. Rev. Lett. **123**, 123601 (2019), doi:[10.1103/PhysRevLett.123.123601](https://doi.org/10.1103/PhysRevLett.123.123601).
- [19] F. Song, S. Yao and Z. Wang, *Non-Hermitian skin effect and chiral damping in open quantum systems*, Phys. Rev. Lett. **123**, 170401 (2019), doi:[10.1103/PhysRevLett.123.170401](https://doi.org/10.1103/PhysRevLett.123.170401).
- [20] Z. Yang and J. Hu, *Non-Hermitian Hopf-link exceptional line semimetals*, Phys. Rev. B **99**, 081102 (2019), doi:[10.1103/PhysRevB.99.081102](https://doi.org/10.1103/PhysRevB.99.081102).
- [21] R. Hamazaki, K. Kawabata and M. Ueda, *Non-Hermitian many-body localization*, Phys. Rev. Lett. **123**, 090603 (2019), doi:[10.1103/PhysRevLett.123.090603](https://doi.org/10.1103/PhysRevLett.123.090603).
- [22] K. Kawabata, T. Bessho and M. Sato, *Classification of exceptional points and non-Hermitian topological semimetals*, Phys. Rev. Lett. **123**, 066405 (2019), doi:[10.1103/PhysRevLett.123.066405](https://doi.org/10.1103/PhysRevLett.123.066405).
- [23] K. Kawabata, S. Higashikawa, Z. Gong, Y. Ashida and M. Ueda, *Topological unification of time-reversal and particle-hole symmetries in non-Hermitian physics*, Nat. Commun. **10**, 297 (2019), doi:[10.1038/s41467-018-08254-y](https://doi.org/10.1038/s41467-018-08254-y).
- [24] C. H. Lee, L. Li and J. Gong, *Hybrid higher-order skin-topological modes in nonreciprocal systems*, Phys. Rev. Lett. **123**, 016805 (2019), doi:[10.1103/PhysRevLett.123.016805](https://doi.org/10.1103/PhysRevLett.123.016805).
- [25] K. Yokomizo and S. Murakami, *Non-Bloch band theory of non-Hermitian systems*, Phys. Rev. Lett. **123**, 066404 (2019), doi:[10.1103/PhysRevLett.123.066404](https://doi.org/10.1103/PhysRevLett.123.066404).

- [26] L. Jin, H. C. Wu, B.-B. Wei and Z. Song, *Hybrid exceptional point created from type-III Dirac point*, Phys. Rev. B **101**, 045130 (2020), doi:[10.1103/PhysRevB.101.045130](https://doi.org/10.1103/PhysRevB.101.045130).
- [27] J. A. S. Lourenço, R. L. Eneias and R. G. Pereira, *Kondo effect in a  $\mathcal{PT}$ -symmetric non-Hermitian Hamiltonian*, Phys. Rev. B **98**, 085126 (2018), doi:[10.1103/PhysRevB.98.085126](https://doi.org/10.1103/PhysRevB.98.085126).
- [28] S. Mu, C. H. Lee, L. Li and J. Gong, *Emergent Fermi surface in a many-body non-Hermitian fermionic chain*, Phys. Rev. B **102**, 081115 (2020), doi:[10.1103/PhysRevB.102.081115](https://doi.org/10.1103/PhysRevB.102.081115).
- [29] N. Okuma and M. Sato, *Topological phase transition driven by infinitesimal instability: Majorana fermions in non-Hermitian spintronics*, Phys. Rev. Lett. **123**, 097701 (2019), doi:[10.1103/PhysRevLett.123.097701](https://doi.org/10.1103/PhysRevLett.123.097701).
- [30] M. V. Berry, *Physics of nonhermitian degeneracies*, Czechoslov. J. Phys. **54**, 1039 (2004), doi:[10.1023/B:CJOP0000044002.05657.04](https://doi.org/10.1023/B:CJOP0000044002.05657.04).
- [31] W. D. Heiss, *The physics of exceptional points*, J. Phys. A: Math. Theor. **45**, 444016 (2012), doi:[10.1088/1751-8113/45/44/444016](https://doi.org/10.1088/1751-8113/45/44/444016).
- [32] M.-A. Miri and A. Alù, *Exceptional points in optics and photonics*, Science **363**, eaar7709 (2019), doi:[10.1126/science.aar7709](https://doi.org/10.1126/science.aar7709).
- [33] X. Zhang and J. Gong, *Non-Hermitian Floquet topological phases: Exceptional points, coalescent edge modes, and the skin effect*, Phys. Rev. B **101**, 045415 (2020), doi:[10.1103/PhysRevB.101.045415](https://doi.org/10.1103/PhysRevB.101.045415).
- [34] J. Doppler et al., *Dynamically encircling an exceptional point for asymmetric mode switching*, Nature **537**, 76 (2016), doi:[10.1038/nature18605](https://doi.org/10.1038/nature18605).
- [35] H. Xu, D. Mason, L. Jiang and J. G. E. Harris, *Topological energy transfer in an optomechanical system with exceptional points*, Nature **537**, 80 (2016), doi:[10.1038/nature18604](https://doi.org/10.1038/nature18604).
- [36] S. Assawaworrarit, X. Yu and S. Fan, *Robust wireless power transfer using a nonlinear parity-time-symmetric circuit*, Nature **546**, 387 (2017), doi:[10.1038/nature22404](https://doi.org/10.1038/nature22404).
- [37] J. Wiersig, *Enhancing the sensitivity of frequency and energy splitting detection by using exceptional points: Application to microcavity sensors for single-particle detection*, Phys. Rev. Lett. **112**, 203901 (2014), doi:[10.1103/PhysRevLett.112.203901](https://doi.org/10.1103/PhysRevLett.112.203901).
- [38] J. Wiersig, *Sensors operating at exceptional points: General theory*, Phys. Rev. A **93**, 033809 (2016), doi:[10.1103/PhysRevA.93.033809](https://doi.org/10.1103/PhysRevA.93.033809).
- [39] H. Hodaei, A. U. Hassan, S. Wittek, H. Garcia-Gracia, R. El-Ganainy, D. N. Christodoulides and M. Khajavikhan, *Enhanced sensitivity at higher-order exceptional points*, Nature **548**, 187 (2017), doi:[10.1038/nature23280](https://doi.org/10.1038/nature23280).
- [40] W. Chen, Ş. K. Özdemir, G. Zhao, J. Wiersig and L. Yang, *Exceptional points enhance sensing in an optical microcavity*, Nature **548**, 192 (2017), doi:[10.1038/nature23281](https://doi.org/10.1038/nature23281).
- [41] C. N. Yang, *Concept of off-diagonal long-range order and the quantum phases of liquid He and of superconductors*, Rev. Mod. Phys. **34**, 694 (1962), doi:[10.1103/RevModPhys.34.694](https://doi.org/10.1103/RevModPhys.34.694).
- [42] L. Jin and Z. Song, *Solutions of  $\mathcal{PT}$ -symmetric tight-binding chain and its equivalent Hermitian counterpart*, Phys. Rev. A **80**, 052107 (2009), doi:[10.1103/PhysRevA.80.052107](https://doi.org/10.1103/PhysRevA.80.052107).

- [43] X. Z. Zhang, L. Jin and Z. Song, *Self-sustained emission in semi-infinite non-Hermitian systems at the exceptional point*, Phys. Rev. A **87**, 042118 (2013), doi:[10.1103/PhysRevA.87.042118](https://doi.org/10.1103/PhysRevA.87.042118).
- [44] L. Jin and Z. Song, *Physics counterpart of the  $\mathcal{PT}$  non-Hermitian tight-binding chain*, Phys. Rev. A **81**, 032109 (2010), doi:[10.1103/PhysRevA.81.032109](https://doi.org/10.1103/PhysRevA.81.032109).
- [45] L. Jin and Z. Song, *Partitioning technique for discrete quantum systems*, Phys. Rev. A **83**, 062118 (2011), doi:[10.1103/PhysRevA.83.062118](https://doi.org/10.1103/PhysRevA.83.062118).
- [46] L. Jin and Z. Song, *A physical interpretation for the non-Hermitian Hamiltonian*, J. Phys. A: Math. Theor. **44**, 375304 (2011), doi:[10.1088/1751-8113/44/37/375304](https://doi.org/10.1088/1751-8113/44/37/375304).